Sulfonated silica/carbon nanocomposites as novel catalysts for hydrolysis of cellulose to glucose†

Stijn Van de Vyver,[a] Li Peng,[a] Jan Geboers,[a] Hans Schepers,[a] Filip de Clippel,[a] Cedric J. Gommes,[b,c] Bart Goderis,[c] Pierre A. Jacobs*[a] and Bert F. Sels*[a]

Received 20th June 2010, Accepted 20th July 2010
DOI: 10.1039/c0gc00235f

Sulfonated silica/carbon nanocomposites were successfully developed as reusable, solid acid catalysts for the hydrolytic degradation of cellulose into high yields of glucose.

With the world's focus on reducing our dependency on fossil fuel resources, one of the challenges faced by future biorefinery processes will be the development of efficient catalysts for selective transformation of cellulosic biomass.[1] The cleavage of β-1,4-glycosidic linkages between cellulose anhydroglucose subunits is of fundamental interest and plays an essential role in the production of plant-derived biofuels and platform chemicals. But while there are many examples of cellulose hydrolysis with mineral acids,[2] heteropolyacids,[3] enzymes,[4] ionic liquids,[5] or hot compressed water,[6] product yields are often limited and several practical limitations are worth mentioning. The use of sulfuric acid, for example, suffers from energy inefficiency and requires a thorough separation, recycling, and treatment of the acid waste residue. On the other hand, aside from their high cost, cellulase enzymes currently need long residence times.

The paucity of recyclable solid materials as a replacement of homogeneous acid catalysts is usually attributed to the low density and strength of the acid sites on their surface.[7] Since the hydrolysis of cellulose is directly correlated to the concentration and pK_a of the acid employed,[1e] efficient catalysts require a high density of accessible and strong Brønsted acid sites with high stability in aqueous environments. In the past few years, considerable progress has been made in the development of such catalysts. Onda *et al.* were the first to study the conversion of ball-mill pretreated cellulose over sulfonated activated carbon catalysts, and they achieved a notable glucose yield of 41%.[8] Suganuma *et al.* investigated the catalytic performance of amorphous carbon bearing SO_3H, COOH, and OH functional groups.[9] The authors reported 68% cellulose conversion after 3 h reaction at 100 °C, yielding 4% glucose and 64% water-soluble β-1,4 glucan. Takagaki *et al.* achieved a combined yield of 9% glucose and cellobiose using layered niobium molybdate ($HNbMoO_6$) as solid catalyst.[10] Another recent development in the field of aqueous-phase cellulose hydrolysis was the extension of this strategy by a transition metal-catalyzed conversion of intermediate oligosaccharides, resulting in 28% yield of glucose on a Ru/CMK catalyst.[11]

In the search for an alternative solid catalyst for cellulose hydrolysis, we report the use of a new class of sulfonated silica/carbon nanocomposite catalysts, capable of achieving high glucose yields compared to reference catalysts and commercial zeolites. The organic part of the hybrid material not only generates flexibility and versatility for further functionalization with *e.g.* acid groups; its silica components also allow good mechanical and thermal stability. The nanocomposites were synthesized by the evaporation-induced triconstituent co-assembly method in order to ensure high entanglement of carbon and silica.[12] Tetraethyl orthosilicate (TEOS) is used as silica precursor, while Pluronic F127 triblock copolymer ($EO_{106}PO_{70}EO_{106}$, M_w = 12600) acts as the structure-directing amphiphilic surfactant. Herein, we used sucrose as a green alternative carbon source instead of the commonly reported noxious phenol resins.[12] Evaporation of the sucrose/silica/F127 solution, followed by carbonization in N_2 atmosphere at 673 K or 823 K decomposes F127 and transforms the sucrose moieties into carbon residues, resulting in nanocomposites containing hydrophobic carbon in close contact with the stabilizing hydrophilic silica matrix. Samples with three different carbon contents, *viz.* 66, 50 and 33 wt%, were prepared by changing the concentration of the sucrose solution added. These hybrid materials were finally treated with sulfuric acid, as described earlier,[13] to obtain the sulfonated silica/carbon nanocomposites, further denoted as SimCn-T-SO_3H (m, n are the weight percentages of silica and carbon, respectively, T is the temperature of carbonization in K).

The small-angle X-ray scattering (SAXS) patterns of the as-synthesized and sulfonated samples are shown in Fig. 1. The SAXS of all samples exhibit a clear maximum at scattering vector q^*, and dim secondary maxima are observed for some samples at larger q values. Although the exact positions of the latter cannot be determined accurately, they overlap nicely with those expected for cylindrical pores being stacked according to a hexagonal (*p6mm*) symmetry, namely $\sqrt{3}\,q^*$ and $2q^*$. The blurriness of the peaks suggests that this hexagonal order is short-ranged. The average distance between neighboring pores is calculated as $a = 4\pi/(\sqrt{3}\,q^*)$, and the corresponding values are reported in Table S1 of the ESI†. Uniform mesopore diameters between 6 to 8 nm were analyzed with N_2 physisorption for

---

[a] *Center for Surface Chemistry and Catalysis, Katholieke Universiteit Leuven, Kasteelpark Arenberg 23, 3001, Heverlee, Belgium. E-mail: bert.sels@biw.kuleuven.be, pierre.jacobs@biw.kuleuven.be; Fax: (+32) 1632 1998; Tel: (+32)1632 1593*

[b] *Department of Chemical Engineering, allée du 6 Août 3, University of Liège B6A, B-4000, Liège, Belgium*

[c] *Department of Molecular and Nanomaterials, Katholieke Universiteit Leuven, Celestijnenlaan 200F, 3001, Heverlee, Belgium*

† Electronic supplementary information (ESI) available: Catalyst preparation; TGA, SAXS, N_2 physisorption and SEM characterization of the sulfonated silica/carbon nanocomposites; properties of zeolite samples used; SEM images, XRD patterns, CP/MAS ^{13}C NMR and IR spectra of the cellulose feed, before and after ball-milling; additional experimental and analytical information. See DOI: 10.1039/c0gc00235f

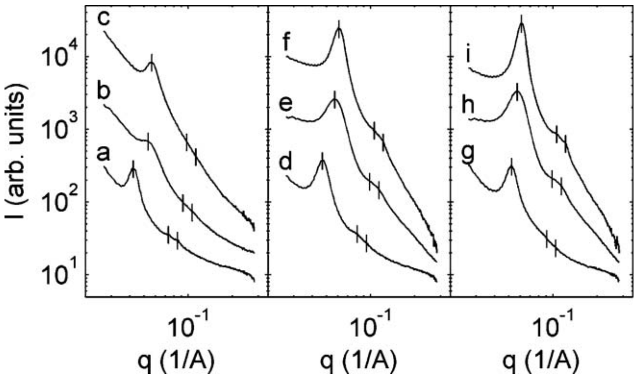

Fig. 1 SAXS patterns of samples (a) Si33C66; (b) Si33C66-673-SO_3H; (c) Si33C66-823-SO_3H; (d) Si50C50; (e) Si50C50-673-SO_3H; (f) Si50C50-823-SO_3H; (g) Si66C33; (h) Si66C33-673-SO_3H; (i) Si66C33-823-SO_3H. The vertical lines indicate the positions of the (1,0), (1,1) and (2,0) scattering peaks of a system having hexagonal symmetry; the values are calculated from the position of the SAXS maximum.

the sulfonated material (Table 1), except for the two carbon-rich samples. Careful analysis of the SAXS data of the latter (b and c, Fig. 1) reveals a lowering in intensity and peak broadening, while the pore structure seems susceptible to pronounced shrinkage (see Δ_a values in Table 1). Such shrinkage has been recognized before,[14] and might be indicative of partial structure collapse.

Initially, acid-catalyzed hydrolysis of cellulose (Sigma-Aldrich; Avicel PH-101, pretreated by ball-milling for 24 h; see ESI†) was explored using a series of ion-exchange resins and commercial zeolites (Fig. 2). Of all these solid acids, macroreticular Amberlyst 15, described earlier as an active hydrolysis catalyst,[1i,1j,5b,5c,8,9] gave the highest yield of 29% glucose, with 57% selectivity. The main side-products analyzed by HPLC in this work were mannose, fructose, levoglucosan, 5-hydroxymethylfurfural (5-HMF) and cello-oligomers. Screening a variety of zeolites revealed limited glucose selectivity even at moderate conversion. The results in Fig. 2 further indicate a difference in activity along the protonated ultrastable zeolite Y samples (USY, CBV series; Table S2, ESI†). The rationale behind these experiments is likely found in the increasing Si/Al ratio in the series from USY CBV 600 to 780, which translates into a decreasing number of Brønsted acid sites with increasing strength.[15–18] At low Si/Al ratios, *viz.* 2.6 for USY CBV 400 and 600, hardly any activity can be discerned. The best results are achieved on a USY CBV 760, suggesting an optimal regime for zeolite acidity, acid strength and accessibility.

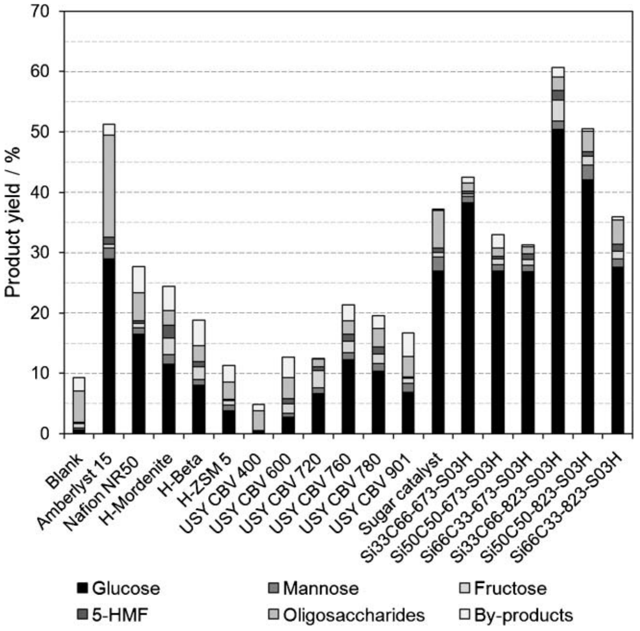

Fig. 2 Hydrolytic conversion of cellulose over heterogeneous acids. Reaction conditions: cellulose pretreated by ball-milling 0.05 g, catalyst 0.05 g, water 5 mL, reaction time 24 h, temperature 423 K.

With this knowledge in mind, we focused on the hydrolytic conversion of cellulose on the new class of sulfonated silica/carbon nanocomposites (Fig. 2). Here, a sulfonated amorphous sugar catalyst, as reported by Toda *et al.*,[19] is taken as a benchmark catalyst, yielding 27% glucose at 37% conversion. Comparatively better results were obtained when the title composites were used. As a first case study, Si33C66-673-SO_3H showed the best performance, combining 38% glucose yield with elevated selectivity (90%). Surprisingly, carbonization of this nanocomposite at higher temperature led to an increase in glucose yield up to 50% for Si33C66-823-SO_3H, which is, to the best of our knowledge, the highest value so far reported for a solid catalyst. Increasing the silica/carbon ratio had a negative effect on the catalytic reaction; that is, both cellulose conversion and glucose yield decreased significantly. When relating these catalytic data to the textural information of Table 1, the requirement of mesoporosity on acid-catalyzed cellulose hydrolysis can be discarded. This experimental observation is in line with our previous notion of restricted space inside micro- and mesoporous systems, preventing micrometer-scaled cellulose particles from penetrating to the active catalytic sites (for SEM images, see the ESI†).[20]

In order to rationally evaluate the performance of the composites, a comparative study is shown in Table 2, including acid density, glucose formation rate and turnover frequency (TOF) at acid sites. The expectations based on titration results in Table 2 are in general agreement with the catalytic observations in that glucose formation is found to occur faster on nanocomposites with higher acid density, even though the values obtained for Si50C50-673-SO_3H and Si66C33-673-SO_3H are fairly close. More interestingly, the TOF data point to the prominent role that the hybrid-structured surface character plays in the hydrolytic activity of the Brønsted acid sites. Indeed, higher TOFs were determined for samples with increased silica/carbon mass ratio, and hence higher hydrophilicity. In previous studies it has been found that efficient conversion of cellulose requires a good interaction between the solid acid catalyst and β-1,4 glucan.[9] In the present case, the above mentioned correlation between catalyst composition and TOF data strongly suggests that the hydrophilic silica groups facilitate substrate adsorption.

The reusability of Si33C66-823-SO_3H, the best catalyst identified in this work, was investigated by filtrating the reaction solution and drying the used catalyst at 373 K between consecutive cycles. Recycling studies showed that the catalyst can be reused several times with only a significant decrease in glucose yield after the first run (Table 3). This initial deactivation might be attributed to the leaching of some polycyclic aromatic hydrocarbon-containing SO_3H groups, as reported earlier for

Table 1 Physicochemical properties of the sulfonated silica/carbon nanocomposites with various carbon contents

Sample	$S_{\mathrm{BET}}{}^{a}$/m^2 g^{-1}	$V_{\mathrm{tot}}{}^{b}$/cm^3 g^{-1}	$V_{\mathrm{meso}}{}^{c}$/cm^3 g^{-1}	$D_{\mathrm{meso}}{}^{d}$/nm	$\Delta_{\mathrm{a}}{}^{e}$/nm
Si33C66-673-SO_3H	471	0.20	0.02	—	3.6
Si50C50-673-SO_3H	424	0.25	0.13	7.6	2.8
Si66C33-673-SO_3H	493	0.44	0.33	6.9	1.2
Si33C66-823-SO_3H	—	—	—	—	4.4
Si50C50-823-SO_3H	124	0.10	0.07	6.9	3.6
Si66C33-823-SO_3H	332	0.39	0.35	6.7	2.0

[a] Surface area (S_{BET}) was calculated by the Brunauer–Emmett–Teller (BET) isotherm method. [b] Total pore volume (V_{tot}) was calculated from the saturation plateau at high relative pressure. [c] Mesopore volume (V_{meso}) was determined according to the *t*-plot method. [d] Average mesopore diameter (D_{meso}) was calculated from adsorption branches of the isotherms, based on the Barett–Joyner–Halenda (BJH) method. [e] Δ_{a} is the average shrinkage between neighboring pores after carbonization, based on SAXS data (for details, see the ESI† Table S1).

Table 2 Hydrolysis of cellulose by a sulfonated amorphous sugar catalyst and sulfonated silica/carbon nanocomposites[a]

Sample	Acid density[b]/ mmol g^{-1}	Formation rate of glucose/μmol h^{-1}	TOF[c]/h^{-1}
Sugar catalyst	0.93	2.98	0.06
Si33C66-673-SO_3H	0.57	4.17	0.15
Si50C50-673-SO_3H	0.40	2.96	0.15
Si66C33-673-SO_3H	0.31	2.97	0.19
Si33C66-823-SO_3H	0.37	5.57	0.30
Si50C50-823-SO_3H	0.25	4.64	0.37
Si66C33-823-SO_3H	0.15	3.05	0.41

[a] Reaction conditions: see Fig. 2. [b] Acid density was determined by automatic titration with an aqueous NaOH solution. [c] TOF = moles glucose formed per mole of acid site per hour.

Table 3 Reusability of the Si33C66-823-SO_3H catalyst system

Entry	Recycle number	Cellulose conversion/%	Glucose yield/%
1	Fresh	60.7	50.4
2	Filtrate solution[a]	11.9	3.7
3	Recycle 1	59.9	44.1
4	Recycle 2	54.3	42.6
5	Recycle 3	55.8	42.5

[a] The solid catalyst and the cellulose residue from the 1st reaction cycle were removed by centrifugation and filtration, before reacting the filtrate solution with a fresh cellulose feed.

sulfonated carbon catalysts.[21] The minor loss of acid groups was further corroborated by reacting the filtrate solution of the first reaction cycle with a fresh cellulose feed (Table 3, entry 2). The conversion of cellulose and yield to glucose were indeed slightly higher than those of the blank reaction in Fig. 2.

In conclusion, sulfonated silica/carbon nanocomposites have been demonstrated to have significant potential for the selective hydrolysis of cellulose into glucose. Their high catalytic performance can be attributed to (i) the presence of strong, accessible Brønsted acid sites and (ii) the hybrid surface structure constituted by interpenetrated silica and carbon components, facilitating the adsorption of β-1,4 glucan on the solid catalyst. Currently, expansion of the catalytic system to include other substrates and applications for lignocellulosic biomass hydrolysis is in progress.

Acknowledgements

This work was performed within the framework of IAP (Belspo), IDECAT and Methusalem (CASAS, long-term financing from the Flemish government) projects. S.V.d.V. is an aspirant of the FWO (Fonds Wetenschappelijk Onderzoek – Vlaanderen), J.G. thanks IWT for a doctoral fellowship and C.J.G. is a postdoctoral fellow of the FRS-FNRS (Belgium).

Notes and references

1 (*a*) D. Klemm, B. Heublein, H. Fink and A. Bohn, *Angew. Chem., Int. Ed.*, 2005, **44**, 3358; (*b*) G. W. Huber, S. Iborra and A. Corma, *Chem. Rev.*, 2006, **106**, 4044; (*c*) G. Centi and R. A. van Santen, *Catalysis for Renewables*, Wiley, Chichester, 2007; (*d*) P. Gallezot, *ChemSusChem*, 2008, **1**, 734; P. Gallezot, *Top. Catal.*, DOI: 10.1007/s11244-010-9564-y; (*e*) R. Rinaldi and F. Schüth, *Energy Environ. Sci.*, 2009, **2**, 610; R. Rinaldi and F. Schüth, *ChemSusChem*, 2009, **2**, 1096; (*f*) V. Jollet, F. Chambon, F. Rataboul, A. Cabiac, C. Pinel, E. Guillon and N. Essayem, *Green Chem.*, 2009, **11**, 2052; (*g*) Y. Wu, Z. Fu, D. Yin, Q. Xi, F. Liu, C. Lu and L. Mao, *Green Chem.*, 2010, **12**, 696; (*h*) Y. Zhang, A. Wang and T. Zhang, *Chem. Commun.*, 2010, **46**, 862; (*i*) W. Deng, M. Liu, Q. Zhang, X. Tan and Y. Wang, *Chem. Commun.*, 2010, **46**, 2668; (*j*) N. Villandier and A. Corma, *Chem. Commun.*, 2010, **46**, 4408; (*k*) J. P. Lange, R. Price, P. M. Ayoub, J. Louis, L. Petrus, L. Clarke and H. Gosselink, *Angew. Chem., Int. Ed.*, 2010, **49**, 4479; (*l*) R. Palkovits, *Angew. Chem., Int. Ed.*, 2010, **49**, 4336; (*m*) D. M. Alonso, J. Q. Bond, J. C. Serrano-Ruiz and J. A. Dumesic, *Green Chem.*, 2010, **12**, 992; (*n*) J. Q. Bond, D. M. Alonso, D. Wang, R. M. West and J. A. Dumesic, *Science*, 2010, **327**, 1110.

2 (*a*) S. Deguchi, K. Tsujii and K. Horikoshi, *Green Chem.*, 2008, **10**, 623; (*b*) M. A. Harmer, A. Fan, A. Liauw and R. K. Kumar, *Chem. Commun.*, 2009, 6610; (*c*) R. Palkovits, K. Tajvidi, J. Procelewska, R. Rinaldi and A. Ruppert, *Green Chem.*, 2010, **12**, 972.

3 (*a*) J. Geboers, S. Van de Vyver, K. Carpentier, K. de Blochouse, P. Jacobs and B. Sels, *Chem. Commun.*, 2010, **46**, 3577; (*b*) K. Shimizu, H. Furukawa, N. Kobayashi, Y. Itaya and A. Satsuma, *Green Chem.*, 2009, **11**, 1627.

4 A. C. Salvador, M. C. Santos and J. A. Saraiva, *Green Chem.*, 2010, **12**, 632.

5 (*a*) S. Zhu, Y. Wu, Q. Chen, Z. Yu, C. Wang, S. Jin, Y. Ding and G. Wu, *Green Chem.*, 2006, **8**, 325; (*b*) R. Rinaldi, R. Palkovits and F. Schüth, *Angew. Chem., Int. Ed.*, 2008, **47**, 8047; (*c*) R. Rinaldi, N. Meine, J. vom Stein, R. Palkovits and F. Schüth, *ChemSusChem*, 2010, **3**, 266; (*d*) I. A. Ignatyev, C. Van Doorselaar, P. G. N. Mertens, K. Binnemans and D. E. De Vos, *ChemSusChem*, 2010, **3**, 91; (*e*) C. Li, Q. Wang and Z. K. Zhao, *Green Chem.*, 2008, **10**, 177; (*f*) L. Vanoye, M. Fanselow, J. D. Holbrey, M. P. Atkins and K. R. Seddon, *Green Chem.*, 2009, **11**, 390; (*g*) X. Qi, M. Watanabe, T. M. Aida and R. L. Smith, *ChemSusChem*, 2010, DOI: 10.1002/cssc.201000124.

6 S. Deguchi, K. Tsujii and K. Horikoshi, *Chem. Commun.*, 2006, 3293; S. Deguchi, K. Tsujii and K. Horikoshi, *Green Chem.*, 2008, **10**, 191; S. Deguchi, K. Tsujii and K. Horikoshi, *Green Chem.*, 2008, **10**, 623.

7 M. Kitano, D. Yamaguchi, S. Satoshi, K. Nakajima, H. Kato, S. Hayashi and M. Hara, *Langmuir*, 2009, **25**, 5068.

8 A. Onda, T. Ochi and K. Yanagisawa, *Green Chem.*, 2008, **10**, 1033; A. Onda, T. Ochi and K. Yanagisawa, *Top. Catal.*, 2009, **52**, 801.

9 (*a*) S. Suganuma, K. Nakajima, M. Kitano, D. Yamaguchi, H. Kato, S. Hayashi and M. Hara, *J. Am. Chem. Soc.*, 2008, **130**, 12787; (*b*) Yamaguchi, M. Kitano, S. Suganuma, K. Nakajima, H. Kato and M. Hara, *J. Phys. Chem. C*, 2009, **113**, 3181.

10 (*a*) A. Takagaki, C. Tagusagawa and K. Domen, *Chem. Commun.*, 2008, 5363; (*b*) A. Takagaki, C. Tagusagawa, S. Hayashi, M. Hara and K. Domen, *Energy Environ. Sci.*, 2010, **3**, 82.

11 H. Kobayashi, T. Komanoya, K. Hara and A. Fukuoka, *ChemSusChem*, 2010, **3**, 440.

12 (*a*) R. Liu, Y. Shi, Y. Wan, Y. Meng, F. Zhang, D. Gu, Z. Chen, B. Tu and D. Zhao, *J. Am. Chem. Soc.*, 2006, **128**, 11652; (*b*) Q. Hu, R. Kou, J. Pang, T. L. Ward, M. Cai, Z. Yang, Y. Lu and J. Tang, *Chem. Commun.*, 2007, 601.

13 L. Peng, A. Philippaerts, X. Ke, J. Van Noyen, F. de Clippel, G. Van Tendeloo, P. A. Jacobs and B. F. Sels, *Catal. Today*, 2010, **150**, 140.

14 M. Imperor-Clerc, P. Davidson and A. Davidson, *J. Am. Chem. Soc.*, 2000, **122**, 11925.

15 D. Barthomeuf, *Mater. Chem. Phys.*, 1987, **17**, 49.

16 W. E. Farneth and R. J. Gorte, *Chem. Rev.*, 1995, **95**, 615.

17 M. J. Remy, D. Stanica, G. Poncelet, E. J. P. Feijen, P. J. Grobet, J. A. Martens and P. A. Jacobs, *J. Phys. Chem.*, 1996, **100**, 12440.

18 P. P. Pescarmona, K. P. F. Janssen, C. Delaet, C. Stroobants, K. Houthoofd, A. Philippaerts, C. De Jonghe, J. S. Paul, P. A. Jacobs and B. F. Sels, *Green Chem.*, 2010, **12**, 1083.

19 M. Toda, A. Takagaki, M. Okamura, J. N. Kondo, S. Hayashi, K. Domen and M. Hara, *Nature*, 2005, **438**, 178.

20 S. Van de Vyver, J. Geboers, M. Dusselier, H. Schepers, T. Vosch, L. Zhang, G. Van Tendeloo, P. A. Jacobs and B. F. Sels, *ChemSusChem*, 2010, **3**, 698.

21 X. Mo, D. E. López, K. Suwannakarn, Y. Liu, E. Lotero, J. G. Goodwin Jr. and C. Lu, *J. Catal.*, 2008, **254**, 332.